A LONG BONE COMPOSITE MODEL

Paulo Pedro Kenedi[1], pkenedi@cefet-rj.br
Ivan Ivanovitsch Thesi Riagusoff[1,2] , ivanthesi@yahoo.com.br

[1]PPEMM - Programa de Pós-Graduação em Engenharia Mecânica e Tecnologia dos Materiais - CEFET/RJ - Av. Maracanã, 229 - Maracanã - RJ - CEP 20271-110 - Brasil

[2]ESSS - Av. Presidente Vargas, 3131 / Sala 1203 - Cidade Nova - RJ - CEP 20210-131 - Brasil

Abstract *A human long bone analytic model is developed taking in account the existence of two bone tissues. An elliptic cross section is used to represent a real long bone medial cross section, with an internal trabecular tissue and an external constant thickness cortical tissue. Mechanics of solids is used, at a basic level, to establish an explicit relationship between static loads and the stresses developed at external cortical bone surface. Also, the results of analytic model are compared with the results of a professional finite element software, used as a reference.*

Keywords: *stress analysis, long bone, analytic model*

1. INTRODUCTION

An analytic composite model for long bones is presented. A real human long bone cross section is modeled by an elliptic form, with constant thickness wall. In this model the existence of two types of bone tissues is recognized, cortical and trabecular, each modeled as homogenous and isotropic material. During the development of the analytic composite model the mathematical manipulations were kept at an introductory level, as well as, the application of the theory of mechanics of solids.

As done at former works (Kenedi, 2009a) and (Kenedi, 2009b), several limiting hypotheses have to be made in order to assure viability of this model. For instance, cortical and trabecular bones, are supposed to be homogenous and isotropic. Loading conditions are static. Loads and restrains are positioned only at extremities of long bones, no side ligaments or muscles are recognized. The analysis is made at medial cross section, therefore far from long bone ends.

Special attention was given to maintain the analytic model expressions as simple as they could be. Instead of generating a reduced set of complex expressions, it was preferred generate an extended set of more simple governing expressions. To simplify the model implementation the expressions were fully developed, avoiding expressions with integrals as in (Kenedi, 2009.b).

A finite element (F.E.) model is implemented, with the utilization of a well known commercial FEM package, to serve as reference. It is set linear and elastic, with little displacements and rotations. Two materials are set, trabecular and cortical tissues, through the utilization of isotropic mechanical properties. The human femur geometry, quite complex, was imported from a real human femur scanned geometry. The utilization of a predetermined path to present the stress, at a chosen cross section, increase the results effectiveness.

2. ANALYTIC MODEL

The analytic model was generated through the implementation of stress analysis of a composite cross section. For cortical tissue it is used a hollow elliptic cross section with constant thickness wall. For trabecular tissue it is used a full elliptic cross section. The model expressions have straightforward application, but its calculations are rather laborious. The utilization of mathematical software, like MathCad, is strictly necessary.

Although mechanics of solids is used in introductory level, the elliptic model of two materials, cortical and trabecular tissues generates a relatively large set of expressions. The model uses two axis systems, a local that accompanies the elliptic cross section angular position and a global that always maintains the same reference angular position.

It is supposed that the loadings were divided between bone tissues, configuring a parallel arrangement. The estimation of axial, bending, transverse shear and torsional stresses, as is shown at section 2.2, is function of several mechanical proprieties ratios, well understood that only isotropic mechanical properties were recognized for cortical and trabecular tissues. The analytic model stresses estimative are done at external surface of a long bone medial cross section. The analytic model also generates principal and maximum shear stresses, which are key variables to implementation of any failure criteria.

2.1 – Equivalent loading at a cross section

Figure 1 shows human femur representation, hypothetical cut at a generic medial section. A static force ***P*** is applied at femur's head, at a distance ***d*** away from the generic medial cross section centre, where equivalent forces and moments are shown.

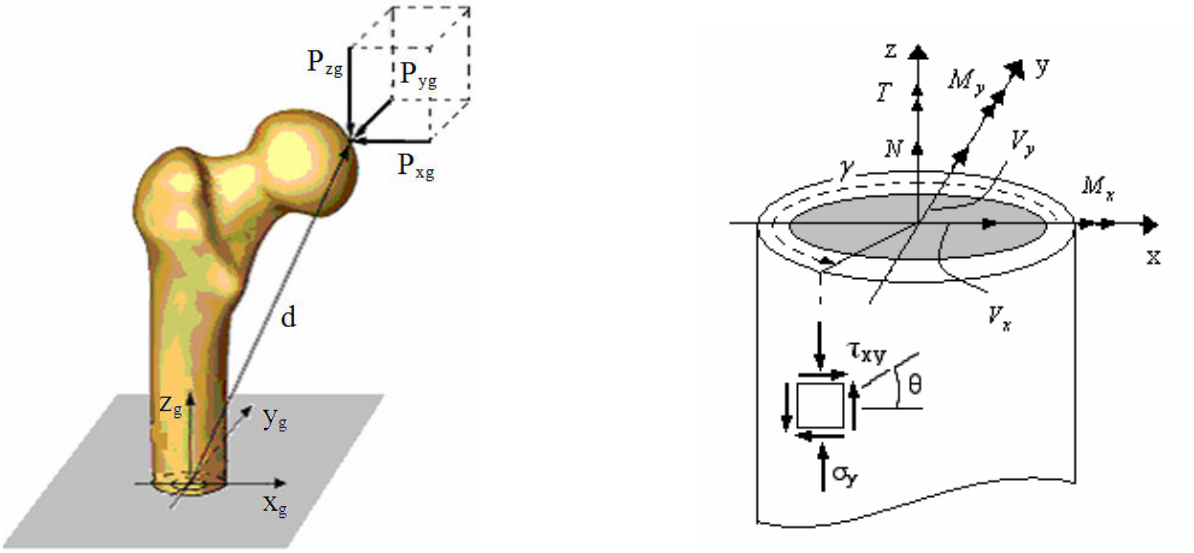

(a) (b)

Figure 1. (a) Static load of a human femur's head and (b) medial cross section equivalent force and moments, in local coordinates.

The static force ***P*** and distance ***d*** are represented by its components in global coordinates system. The force and moments components, at the chosen medial cross section, in global coordinates are:

$$\boldsymbol{P} = P_{xg}\vec{i} + P_{yg}\vec{j} + P_{zg}\vec{k} \quad \text{and} \quad \boldsymbol{d} = d_{xg}\vec{i} + d_{yg}\vec{j} + d_{zg}\vec{k} \tag{1}$$

$$\begin{pmatrix} V_{xg} \\ V_{yg} \\ V_{zg} \end{pmatrix} = \begin{pmatrix} P_{xg} \\ P_{yg} \\ P_{zg} \end{pmatrix} \quad \text{and} \quad \begin{pmatrix} M_{xg} \\ M_{yg} \\ M_{zg} \end{pmatrix} = \begin{pmatrix} d_{yg}P_{zg} - d_{zg}P_{yg} \\ d_{zg}P_{xg} - d_{xg}P_{zg} \\ d_{xg}P_{yg} - d_{yg}P_{xg} \end{pmatrix} \tag{2}$$

Where, the variables presented in bold-faced letters are vectors, the vectors components with *g* subscripts are referenced to global system coordinates. *N* is the axial force, *V* is the shear force, *M* is the bending moment and *T* is the torsional moment. $\vec{i}$, $\vec{j}$ and $\vec{k}$ are unit vectors. Note that $V_{zg} = N$, $M_{zg} = T$. The forces and moments components, written in local coordinates, are:

$$\begin{pmatrix} V_x \\ V_y \\ V_z \end{pmatrix} = \begin{pmatrix} P_{xg}\cos(\varphi) + P_{yg}\sin(\varphi) \\ -P_{xg}\sin(\varphi) + P_{yg}\cos(\varphi) \\ P_{zg} \end{pmatrix} \quad \text{and} \quad \begin{pmatrix} M_x \\ M_y \\ M_z \end{pmatrix} = \begin{pmatrix} M_{xg}\cos(\varphi) + M_{yg}\sin(\varphi) \\ -M_{xg}\sin(\varphi) + M_{yg}\cos(\varphi) \\ M_{zg} \end{pmatrix} \tag{3}$$

The force (3.a) and the moments (3.b) components, written in local coordinates, are represented at Figure 1.b. The angle between global and local coordinates is φ. Note that the φ angle is different for each distance ***d***, because each medial cross section of a human femur bone has a different orientation.

2.2 - Expressions of composite analytic model

Former work estimates the stress distribution at external surface of a medial hollow elliptic cross section of a cortical long bone (Kenedi, 2009b). In this work the analytic composite model, besides cortical external tissue, also consider a trabecular internal tissue. Figure 2, shows the geometry and the coordinate systems of the composite analytic model.

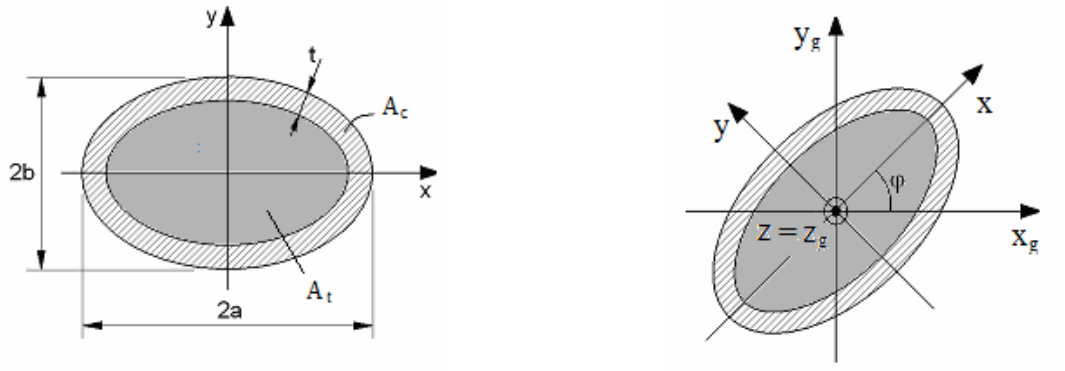

(a) (b)

Figure 2. (a) Idealized composite elliptic cross section and (b) local and global coordinate systems.

Figure 2.a shows a composite elliptic cross section. It has constant thickness wall *t*, with long axis *2a* and short axis 2*b*. The cortical and trabecular cross sectional tissue areas are respectively A_c and A_t. Figure 2.b shows two coordinates systems, local and global. The local coordinates (x,y,z) are attached to cross section, where x and y axis are respectively, coincident with *2a* and *2b* axis. The z axis is obtained by *right-hand rule*. In other words, each cross section has its own local axis configuration, always maintaining x axis coincident with *2a* axis. Global coordinates (x_g,y_g,z_g) has always the same orientation in space, where $x_g y_g$ is the horizontal plane, x_g,z_g and y_g,z_g are vertical planes.

Figures 1.b, 3 and 5.a shows the angle γ, that locates the point of interest angular position, at external bone surface, referred to x axis. The angle θ represents the element of area orientation (at Figure 1.b, $\theta = 0°$) at external bone surface.

Figure 3 shows the composite analytic model bending and transverse shear variables.

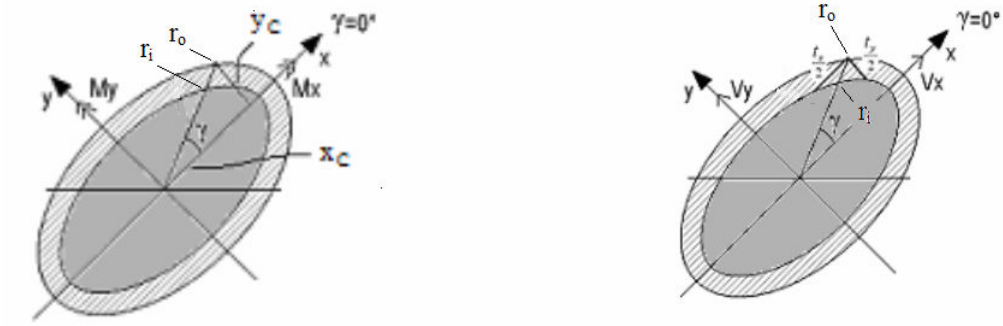

(a) (b)

Figure 3. Composite elliptic cross section: (a) Bending and (b) transverse shear variables.

The analytic model expressions will be presented in following sequence: axial and bending normal stresses; torsional and transverse shear stresses.

It is supposed that cortical and trabecular tissues are in coaxial arrangement, sharing axial load N. The cortical and trabecular axial stress components, respectively, σ_{NC} and σ_{NT}, are (Crandall, 1978):

$$\sigma_{NC} = \frac{N}{A_C + \frac{A_T}{n}} \qquad \text{and} \qquad \sigma_{NT} = \frac{N}{nA_C + A_T} \tag{4}$$

$$\text{where, } A_C = \pi t\left(a + b - t\right) \qquad \text{and} \qquad A_T = \pi\left(a - t\right)\left(b - t\right) \qquad \text{and} \qquad n = \frac{E_C}{E_T} \tag{5}$$

Where the longitudinal modulus of elasticity of cortical and trabecular tissues are, respectively, E_C and E_T. The ratio between the two modulus of elasticity is n.

The bending theory was developed for a homogeneous cross section. For a composite cross section, is usual to "transform" the different materials in only one material (Beer, 2006). The cortical bending stresses components, σ_{BC_x} and σ_{BC_y}; and trabecular bending stresses components σ_{BT_x} and σ_{BT_y} are estimated (Crandall, 1978):

$$\sigma_{BC_x} = \frac{M_x y_C(\gamma)}{I_x} \quad \text{and} \quad \sigma_{BC_y} = -\frac{M_y x_C(\gamma)}{I_y} \quad \text{and} \quad \sigma_{BT_x} = n\frac{M_x y_T(\gamma)}{I_x} \quad \text{and} \quad \sigma_{BT_y} = -n\frac{M_y x_T(\gamma)}{I_y} \tag{6}$$

where,
$$x_C(\gamma) = r_o(\gamma)\cos(\gamma) \quad \text{and} \quad y_C(\gamma) = r_o(\gamma)\sin(\gamma) \quad \text{and} \quad r_o(\gamma) = \frac{ab}{\sqrt{a^2\sin^2(\gamma) + b^2\cos^2(\gamma)}} \tag{7}$$

$$x_T(\gamma) = r_i(\gamma)\cos(\gamma) \quad \text{and} \quad y_T(\gamma) = r_i(\gamma)\sin(\gamma) \quad \text{and} \quad r_i(\gamma) = \frac{(a-t)(b-t)}{\sqrt{(a-t)^2\sin^2(\gamma) + (b-t)^2\cos^2(\gamma)}} \tag{8}$$

$$I_x = \frac{\pi}{4}ab^3 + \frac{4}{3}\left[(a-t)(b-t)^3(n-1)\right] \quad \text{and} \quad I_y = \frac{\pi}{4}a^3b + \frac{4}{3}\left[(a-t)^3(b-t)(n-1)\right] \tag{9}$$

Where, $x_C(\gamma)$ and $y_C(\gamma)$ are, respectively, the perpendicular distances from axis y and x to external cortical bone surface and $x_T(\gamma)$ and $y_T(\gamma)$ is the same to the internal cortical bone surface. I_x and I_y are second moments of area. $r_o(\gamma)$ and $r_i(\gamma)$ are, respectively, the outer and inner radius (shown at Figure 3). Figure 4 shows the transformed section model for trabecular to cortical tissue used to generate second moments of area expressions:

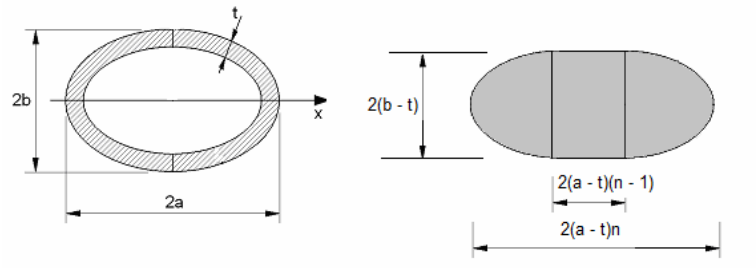

(a)

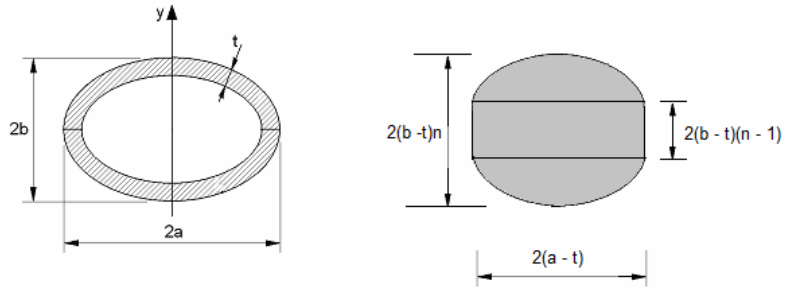

(b)

Figure 4. Transformed section model from trabecular to cortical tissue with respect to: (a) x-axis and (b) y-axis.

To estimate cortical and trabecular torsional stress components, respectively, τ_{TC} and τ_{TT}, it was supposed that cortical and trabecular tissues were in a coaxial arrangement, sharing the torsional moment T (Craig, 2003):

$$\tau_{TC} = \frac{1}{2t\mathrm{A}(1 + (1/pq))}T \quad \text{and} \quad \tau_{TT} = \frac{r_i(\gamma)}{J_T(1+pq)}T \tag{10}$$

$$\text{where, } J_C = \frac{\pi a^3 b^3}{a^2 + b^2} - J_T \quad \text{and} \quad J_T = \frac{\pi(a-t)^3(b-t)^3}{(a-t)^2 + (b-t)^2} \tag{11}$$

$$p = \frac{J_C}{J_T} \quad \text{and} \quad q = \frac{G_C}{G_T} \quad \text{and} \quad \mathrm{A} = \pi\left(a - \frac{t}{2}\right)\left(b - \frac{t}{2}\right) \tag{12}$$

Where, the cortical and trabecular bone polar second moments of area are, respectively, J_C and J_T. The cortical and trabecular bone shear modulus are, respectively, G_C and G_T. The area inside a line which passes in middle thickness wall of cortical bone cross sectionis is A. The ratio between two polar second moments of area is p and the ratio between two shear modulus is q.

The transverse shear theory was developed for a homogeneous cross section. For a composite cross section, is usual to "transform" the different materials in only one material (Craig, 2003). The cortical transverse shear stress components, τ_{VC_x} and τ_{VC_y}; and trabecular transverse shear stress components, τ_{VT_x} and τ_{VT_y}, were estimated as:

$$\tau_{VCx} = \frac{Q_{yc}V_x}{t_{yc}I_y} \quad \text{and} \quad \tau_{VCy} = \frac{Q_{xc}V_y}{t_{xc}I_x} \quad \text{and} \quad \tau_{VTx} = n\frac{Q_{yt}V_x}{t_{yc}I_y} \quad \text{and} \quad \tau_{VTy} = n\frac{Q_{xt}V_y}{t_{xc}I_x} \tag{13}$$

where,

$$t_{xc} = 2a\sqrt{1-\left(\frac{y_C(\gamma)}{b}\right)^2} - t_{xt}k_x \text{ and } t_{yc} = 2b\sqrt{1-\left(\frac{x_C(\gamma)}{a}\right)^2} - t_{yt}k_y \text{ and } t_{xt} = 2(a-t)\sqrt{1-\left(\frac{y_C(\gamma)}{b-t}\right)^2} \text{ and } t_{yt} = 2(b-t)\sqrt{1-\left(\frac{x_C(\gamma)}{a-t}\right)^2} \tag{14}$$

$$Q_{xc} = \frac{2}{3}\left\{\frac{a}{b}\left(b^2 - y_C(\gamma)^2\right)^{3/2} + \left[\left(\frac{a-t}{b-t}\right)\left[(b-t)^2 - y_C(\gamma)^2\right]^{3/2}\right]k_x\right\} \text{ (} k_x = 0 \text{ for } |y_C| \geq (b-t), \; k_x = 1 \text{ otherwise)} \tag{15}$$

$$Q_{yc} = \frac{2}{3}\left\{\frac{b}{a}\left(a^2 - x_C(\gamma)^2\right)^{3/2} + \left[\left(\frac{b-t}{a-t}\right)\left[(a-t)^2 - x_C(\gamma)^2\right]^{3/2}\right]k_y\right\} (k_y = 0 \text{ for } |x_C| \geq (a-t), \; k_y = 1 \text{ otherwise})$$

$$Q_{xt} = \frac{2}{3}\left(\frac{a-t}{b-t}\right)\left[(b-t)^2 - y_T(\gamma)^2\right]^{3/2} + (a-t)(n-1)\left[(b-t)^2 - y_T(\gamma)^2\right]$$

$$Q_{yt} = \frac{2}{3}\left(\frac{b-t}{a-t}\right)\left[(a-t)^2 - x_T(\gamma)^2\right]^{3/2} + (b-t)(n-1)\left[(a-t)^2 - x_T(\gamma)^2\right]$$

Where, Q_{xc}, Q_{yc}, Q_{xt} and Q_{yt} are first moments of area, t_{xc}, t_{yc}, t_{xt} and t_{yt} are thicknesses.

2.3 – Mohr Circle

Using Mohr circle approach is possible to transform non-principal stresses in principal and maximum shear stresses. The resultant of normal and shear stresses can be estimated as shown at (16) and (17) expressions:

$$\sigma_y = \sigma_{NC} + \sigma_{BC} \text{ and } \tau_{xy} = \tau_{TC} + \tau_{VC} \tag{16}$$

$$\text{where, } \sigma_{BC} = \sigma_{BC_x} + \sigma_{BC_y} \text{ and } \tau_{VC} = \tau_{VC_x} + \tau_{VC_y} \tag{17}$$

The principal stresses and angles at surface of a long bone are:

$$\sigma_1, \sigma_3 = \frac{\sigma_y}{2} \pm \sqrt{\left(\frac{\sigma_y}{2}\right)^2 + \tau_{xy}^2} \quad \text{and} \quad \theta = \frac{1}{2}\arctan\left(\left|\frac{2\tau_{xy}}{\sigma_y}\right|\right) \tag{18}$$

The maximum shear stress and angles at surface of a long bone are:

$$\tau_{\max} = \sqrt{\left(\frac{\sigma_y}{2}\right)^2 + \tau_{xy}^2} \quad \text{and} \quad \theta' = \theta + 45^\circ \; or \; \theta' = \theta + 135^\circ \tag{19}$$

Figure 5.b shows a Mohr circle for three angular orientations numbered from 1 to 3, at same external surface point.

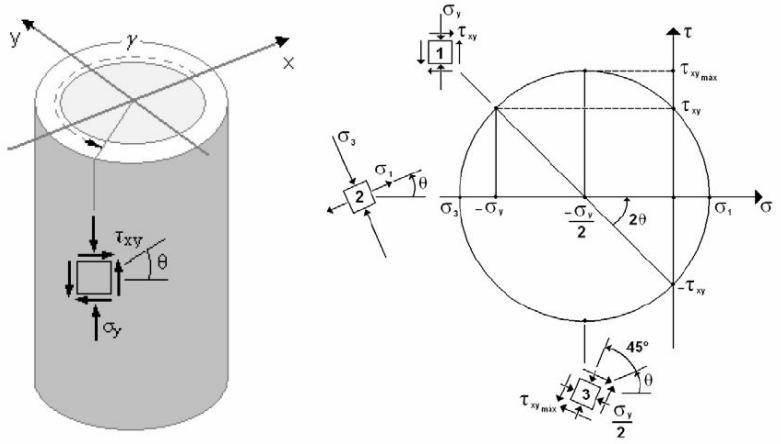

(a) (b)

Figure 5. (a) Element of area at a point of interest at a medial bone surface and (b) Mohr circle.

The first angular orientation corresponds to the actual situation shown at Figure 5.a. The second angular orientation turns θ at external surface of long bone from its initial position (2θ at Mohr circle) to reach the angle of principal stresses. The third angular orientation, add 45° to second position (add 90° at Mohr circle) to reach the angle of maximum shear stresses. Note that at Mohr circle the angle θ is doubled (Crandall, 1978).

2.4 – Analytic Results

Figure 6 shows curves generated with the application of (1)-(19) expressions. At Figure 6 all graphics abscissa shows a complete turn of γ angle at external or internal cortical tissue surfaces, at a medial section of a long bone. The geometric and load data were the same of former work (Kenedi, 2009b).

Some material properties were picked from technical literature as (Rapoff, 2007) and (Rincón-Kohli, 2009): $E_{cortical}$ = 20 GPa, $\nu_{cortical}$ = 0.235 and $E_{trabecular}$ = 18 GPa, $\nu_{trabecular}$ = 0.181. Other material properties were estimated as: $G_{cortical}$ = 8.1 GPa and $G_{cortical}$ = 7.6 GPa to maintain bulk modulus positive.

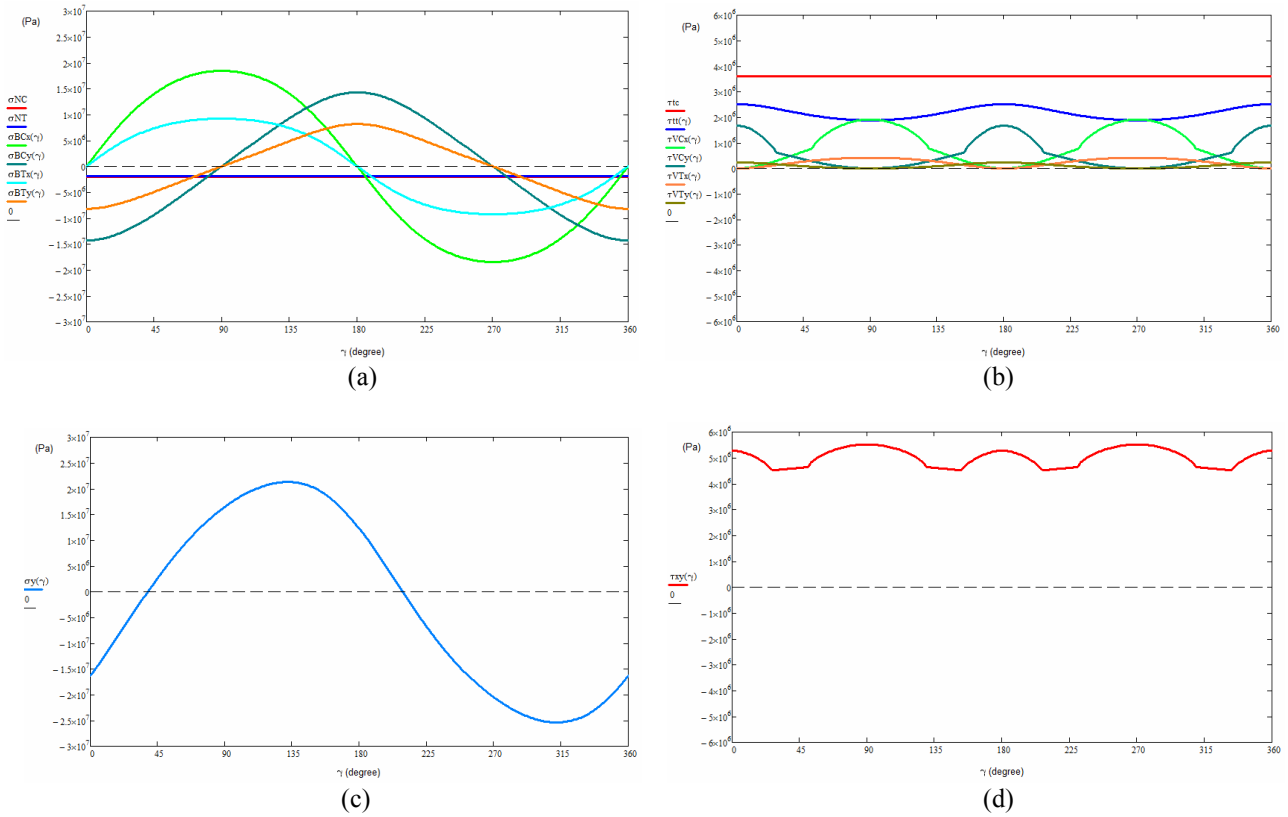

Figure 6. Graphical representation of: (a) Normal stress components, (b) shear stresses components, (c) cortical combined normal stress and (d) cortical combined shear stress.

Note that vertical scale of Figures 6.a and 6.c are bigger than ones of Figures 6.b and 6.d. At Figure 6.a and 6.b both cortical and trabecular stress components are represented for didactic reasons. At Figures 6.c and 6.d only cortical combined normal and shear stresses are represented. Indeed Figures 6.c and 6.d are, respectively, the graphical representation of expressions (16.a) and (16.b).

Analyzing Figures 6.a and 6.b it is clear that the stress components at cortical tissue are larger than stress components at trabecular tissue. Comparing Figures 6.c and 6.d, is apparent that normal stresses are bigger than shear stresses.

Although is almost indistinguishable Figure 6.a shows different values for σ_{NC} and σ_{NT} axial stresses, for cortical and trabecular tissues. Figure 6.b shows a cortical torsional stress, modeled as constant, and a variable trabecular torsional stress. Also at Figure 6.b, the curve smoothness of cortical transverse shear stress components are affected by the elliptic form, changing when the thickness reach the interface between full and hollow section.

3. FINITE ELEMENT MODEL

A finite element model was implemented, with the utilization of a well known commercial F.E. package. The model results were used as reference to composite analytic model. The geometry was imported into ANSYS Design Modeler from a Parasolid file format. Figure 7.a shows a representation of cortical tissue, Figure 7.b shows a representation trabecular tissue and Figure 7.c shows a representation of the composite model, with cortical and trabecular tissues joinned together.

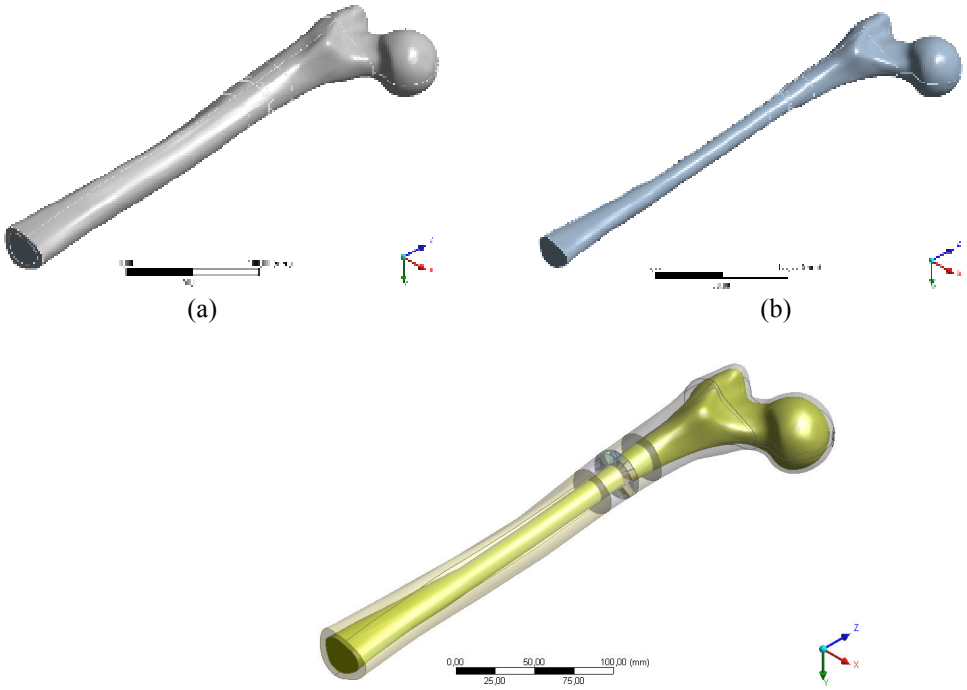

(a) (b)

(c)

Figure 7. F.E. human femur model: (a) cortical tissue, (b) trabecular tissue, (c) composite model, with cortical and trabecular tissues.

The F.E. model of a human femur is linear and elastic, with little displacements and rotations. The geometry is quite complex, but could be imported from a real scanned human femur geometry. Figure 8.a shows the mesh of geometric model and Figure 8.b shows an example of longitudinal stress post-processing result. For this F.E. model was used 62375 Nodes and 38290 Elements (SOLID186 and SOLID187).

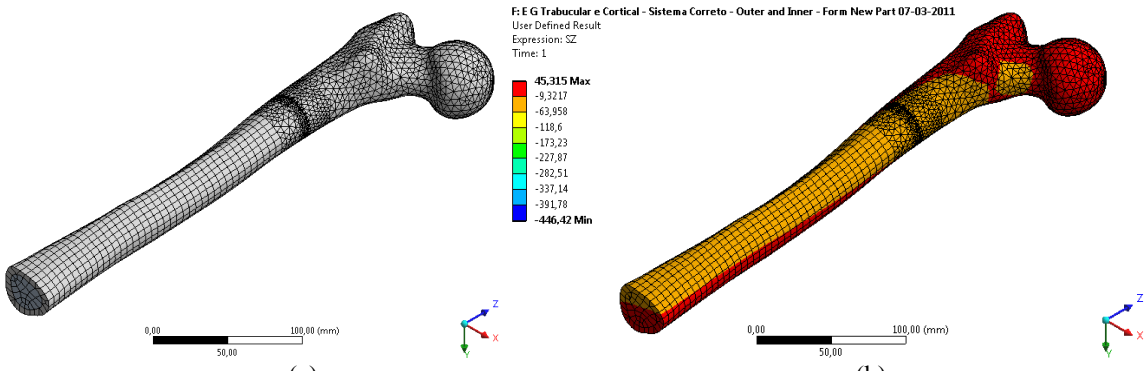

(a) (b)

Figure 8. Human femur finite element model: (a) mesh and (b) longitudinal stress (SZ).

Figure 8.b shows an usual way of longitudinal stress representation (parallel do Z axis) at external surface of cortical tissue, which not gave many details about the stress distribution at a specific area.

An alternative way of stress representation is shown at Figure 9. A path is created at a chosen cross section, where the stress variations can be readily accessed. Evidently the stresses of every node of each path can be also listed.

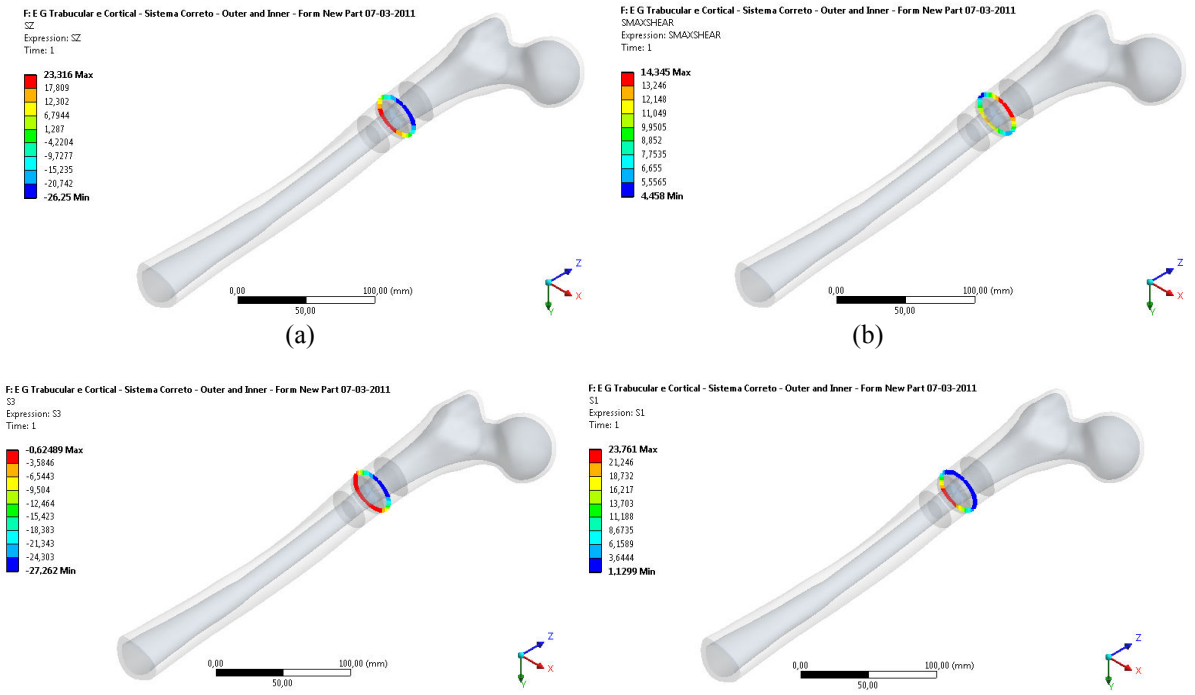

Figure 9. F.E. model results: (a) longitudinal, (b) maximum shear, (c) minimum principal and (d) maximum principal stresses.

Note that each path are, at the same cross section, at external surface of cortical tissue. The stresses level mantain under 30 MPa at external cortical tissue surface. At Figure 9.a, the longitudinal stresses shows that the stress distribution agree with the prevalence of bending stress in comparison with pure axial stress.

4. COMPARATIVE STUDY

The results of the composite analytic model expressions are compared with the results of F.E. model at Figure 10.

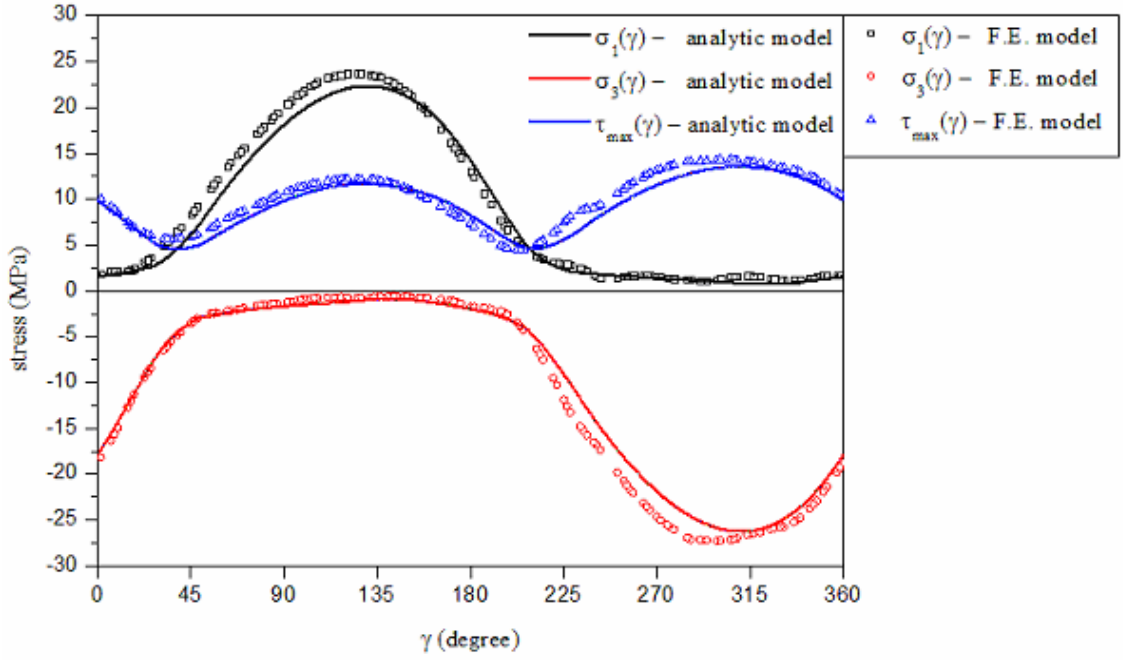

Figure 10. Comparative diagram of results: analytic and F.E. models.

Figure 10 shows the results of principal and maximum shear stresses (σ_1, σ_3 and τ_{max}) for points positioned in a path at external surface of a human femur medial cross section. As the maximum and the minimum principal stresses are opposite in sign, as can be also seen qualitatively at Figure 5.b, the maximum shear stress is the average value between maximum and minimum principal stresses. The results of two models, F.E. (used as reference) and the composite analytic model, are plotted resulting in a close match.

5. CONCLUSIONS

A simple composite analytic model was developed, with limiting hypothesis, to describe the stress distribution, normal and shear componentes, at external surface of a human long bone medial cross section. Principal and maximum shear stresses are also calculated. The performance of analytic model was improved in comparison to former models by the utilization of two bones tissues, cortical and trabecular. The estimative of principal and maximum shear stresses at external surface of long bones, which are key variables to implementation of any failure criteria, are the major goal of this work.

6. REFERENCES

Bayraktar, H.H. et al., 2004, “Comparison of the elastic and yield properties of human femoral trabecular and cortical bone tissue”, J. Biomech., Vol. 37, pp. 27-35.

Beer, F. P., 2006, “Mechanics of Materials”, Fourth Edition in SI units, Mc Graw Hill Education.

Bergmann, G. et al., 2001, “Hip contact forces and gait patterns from routine activities”, J. Biomech., Vol. 34, pp.859-871.

Cilingir, A.C. et al., 2007, “Three-Dimensional Anatomic Finite Element Modeling of Hemi-Arthroplasty of Human Hip Joint”, Trends Biomater. Artif. Organs.., Vol. 21, No. 1, pp. 63-72.

Craig Jr., R.R., 2003, "Mecânica dos Materiais", Segunda Edição, LTC.

Crandall, S.H., Dahl, N. C. and Lardner, T. J., 1978, “An Introduction to the Mechanics of Solids”, Second Edition with SI units, McGraw Hill International Editions.

Doblaré, M., García J. M. and Gómez, M. J., 2004, “Modeling bone tissue fracture and healing: a review”, Engineering Fracture Mechanics, Vol. 71, pp. 1809-1840.

Jones, R.M., 1999, “Mechanics of Composite Materials”, 2nd Edition, Taylor & Francis.

Kenedi, P.P., Riagusoff, I.I.T., 2009b, “Stress Analysis Models of Human Long Bones – Analytic and Finite Analysis Approaches”, In: Proceedings of 20th International Congress of Mechanical Engineering - COBEM 2009, Gramado, Rio Grande do Sul, 10-15 Nov.

Kenedi, P.P., Riagusoff, I.I.T., 2009a, “Analytic and finite element models of a human long bone”, In: Anais do 2° Encontro Nacional de Engenharia Biomecânica, ENEBI 2009, Florianópolis, Santa Catarina, 6-8 Mai.

Karam, L.Z., 2009, "Caracterização de um Fêmur Sintético empregando o Método dos Elementos Finitos e Validação por Extensômetria Ótica", Dissertação de Mestrado, UTFPR, Curitiba, Brasil.

Keyak, J. H., Rosi, S.A., 2000, “Prediction of femoral fracture load using finite element models: an examination of stress – and strain-based failure theories”, J. Biomech., Vol. 33, pp. 209-214.

Liu, X S, et al., 2006, “A 3D Morphological Analysis of Trabecular Bone based on Individual Trabecular Segmentation”, 52nd Annual Meeting of the Orthopaedic Research Society, Chicago, USA.

Patnaik, S. and Hopkins, D., 2004, “Strength of Materials: A Unified Theory”, Elsevier.

Petrtyl, M., Herf, J. and Fiala, P., 1996, “Spatial Organization of the Haversian Bone in Man”, J. Biomech., Vol. 29, No. 2, pp. 161-169.

Rapoff, A.J., 2007, http://engineering.union.edu/~rapoffa/MER440/MER440.htm.

Rincón-Kohli, L. and Zysset, P.K., 2009, "Multi-axial Mechanical Properties of Human trabecular Bone", Biomech Model Mechanobiol, 8, pp. 195-208.

Rudman, K.E. et al., 2006, “Compression or tension? The stress distribution in the proximal femur”, Biomedical Engineering Online, vol.5, No.12.

Sadd, M.H., 2005, “Elasticity – Theory, Applications and Numerics”, Elsevier.

Sommers, M.B. et al., 2007, " A surrogate long-bone model with osteoporotic material properties for biomechanical testing of fracture implants", Journal of Biomechanics, Vol. 40, pp.3297-3304.

Spiegel, M.R., 1992, “Manual de Fórmulas, Métodos e Tabelas de Matemática”, 2º Edição, Makron Books.

Turner, C.H. et al., 1999, “The elastic properties of trabecular and cortical bone tissues are similar: results from two microscopic measurement techniques”, J. Biomech., Vol. 32, Technical Note, pp. 437-441.

7. RESPONSIBILITY NOTICE

The authors are the only responsible for the printed material included in this paper.